A Robust Localization Method for Unmanned Surface Vehicle (USV) Navigation Using Fuzzy Adaptive Kalman Filtering

WENWEN LIU[ID], YUANCHANG LIU, AND RICHARD BUCKNALL

Department of Mechanical Engineering, University College London, London WC1E 7JE, U.K.

Corresponding author: Wenwen Liu (w.liu.11@ucl.ac.uk)

ABSTRACT Recently, multi-sensor navigation has emerged as a viable approach in autonomous vehicles' development. Kalman filtering has been widely applied in multi-sensor data fusion, and researchers are trialing variants of the Kalman Filter (KF) to improve the operational robustness of vehicles in a range of environments under varying dynamic constraints. This paper proposes a novel sensor data fusion algorithm employing an Unscented Kalman Filter (UKF) for the autonomous navigation of an Unmanned Surface Vehicle (USV). Since the navigational sensors on-board the USV are subject to operational uncertainties caused by equipment limitations and environmental disturbances, an improved UKF algorithm with the capability of adaptive estimation, namely fuzzy adaptive UKF data fusion algorithm, has been proposed to obtain reliable navigational information. The conventional UKF is capable of fusing a number of raw sensor measurements and generating relatively accurate estimations with proper *a priori* knowledge of system noise. To deal with systems that lack such information, a fuzzy adaptive estimation method is introduced to enhance the performance of the conventional UKF, making the algorithm capable of verifying and correcting the associated sensor noise in real time. The proposed fuzzy adaptive UKF data fusion algorithm has been tested and evaluated in different simulations modeled using practical maritime environments and the results are compared with the conventional UKF. The sensor measurements taken from a practical USV trial have also been applied to the proposed algorithm for further validation.

INDEX TERMS Unscented Kalman Filter (UKF), adaptive estimation, USV navigation, fuzzy logic, multi-sensor data fusion.

I. INTRODUCTION

In recent years, Unmanned Surface Vehicles (USVs) have gained increasing prominence driven by their ability to carry out unmanned missions on ocean exploration and protection. While undertaking these missions, autonomous navigation of a USV can be crucial. Benefiting from the rapid advancements in navigational devices, such as the Global Positioning System (GPS) and other marine electronics, real-time navigational data can be obtained by an autonomous navigation system without human interaction. However, sensors working as standalone devices cannot provide reliable navigational data since they suffer from loss of signal and uncertainties

The associate editor coordinating the review of this manuscript and approving it for publication was Bo Li.

caused by environmental disturbances and equipment limitations. To address these challenges, one popular approach is to use the multi-sensor data fusion methodology by integrating various sensors as complementary devices. The implementation of multi-sensor navigation relies on effective data fusion algorithms to manage large amounts of raw sensor measurements and deliver reasonably accurate navigational information.

The Kalman Filter (KF) is a popular technique applied to data fusion algorithms as an optimal estimator for linear stochastic systems [1], [2]. However, the marine environment is uncertain and complex for USV navigation. Various aspects could cause position offset, especially environmental influences. Tidal current, wind and waves are the most significant effects that would cause drifting of a moving

water surface vehicle. In this context, the trajectory of an USV is complicated which cannot be simply characterized as operating on a straight line or a curved line in practice. Besides, multi-sensor integration may introduce increased nonlinearity to the system, which is beyond the capability of the conventional KF [3]. Thus, Kalman Filter variants such as the Unscented Kalman Filter (UKF) have been developed and used to deal with non-linear systems. The UKF employs the unscented transform (UT) to approximate the non-linear system [4]–[8]. It first forms a set of Sigma points, which are able to capture exactly the mean and covariance of the original distribution of the system states, and propagates them through the actual non-linear function characterizing the system dynamics. The mean and error covariance of the system states are then recalculated based on the propagated points, yielding more accurate results [9].

Driven by the nature of Kalman filtering, data fusion algorithms based on conventional UKF require accurate *a priori* knowledge on the characteristics of system noise [10]. In particular, the uncertainties in system processing noise and measurement noise have a large impact on the conventional UKF, thereby resulting in degraded performance [11], [12]. An adaptive estimation algorithm to match the system processing noise covariance Q and measurement noise covariance R is a solution to accommodate the influences caused by inaccurate *a priori* knowledge of characteristics of system noise and contributing to a more robust system. The adaptive estimation algorithm is able to determine the system noise covariance of the dynamic system so that the UKF data fusion algorithm can approximate the system state based upon the determined real-time statistical parameters together with the observed data.

Wang et al. [13] proposed a fuzzy logic based adaptive KF algorithm to adapt the two noise parameters to determine the attitudes of a satellite. The algorithm defines an adjustment coefficient according to the designed fuzzy logic system to update the processing error covariance and measurement error covariance for the next state. Jin et al. [14] proposed a fuzzy logic based adaptive estimation method to correct the measurement noise covariance in the KF operation for the inertial motion capture system. Rahimi et al. [15] extends the adaptive research onto the conventional UKF and details the matching between the theoretical and actual processing and measurement error covariance for the applications of reaction wheels. These studies on various practical applications demonstrate the validation and effectiveness of the adaptive estimation for conventional KF/UKF based algorithms.

Previous effort has also been made in the field of navigation. Almagbile et al. [16] demonstrated the performance of covariance matching based adaptive KF methods with different adaptations of the processing error covariance matrix and measurement error covariance matrix. The results suggest that the Q adaptation has impaired filtering accuracy compared to the R adaptation. Meng et al. [17] deduced an adaptive estimating algorithm based on the UKF for both Q

and R adapting simultaneously and applied it to the Global Navigation Satellite System (GNSS) and Inertial Navigation System (INS) hybrid navigation system. However, their method to determine the real-time R matrix is achieved by simply adjusting its theoretical value to the calculated actual value. Compared to the processing error, measurement noise, which is prone to alteration, have a greater impact on the performance of data fusion algorithms since the practical condition of the sensors is difficult to predict and evaluate, detrimentally affecting the data fusion algorithms.

Previous work on adaptive estimations mainly concentrate on combining them with the conventional KF. Given the superior performance of UKF over the conventional KF, this paper fills this knowledge gap by proposing an improved adaptive UKF algorithm that can be applied to robust USV navigation in a practical maritime environment. The novelty of this method lies in the fact that a fuzzy logic based, noise covariance adaptive estimation is developed to compensate sensors' noise and improve the overall performance of estimating a USV's navigational data.

This paper is organized as follows. Section II introduces the details of modelling the movement of an USV. Section III demonstrates how a conventional UKF can be used to improve the accuracy of raw sensor measurements. Section IV specifically details the proposed fuzzy covariance matching adaptive estimation algorithm. Section V validates the algorithm through a number of simulations in practical maritime environments and practical USV trial data. The final section provides the conclusion remarks as well as suggestions for future work.

II. DATA FUSION FOR USV NAVIGATION

Before introducing the UKF algorithm to deal with sensor uncertainties, it is important to establish appropriate system equations to detail the USV's movement. This is because the success of the KF (especially the conventional KF) is largely dependent on accurate system expression [18]. For an autonomous USV navigation, information including its position (p), velocity (v) and heading (θ) is required in real time, which can be calculated by using the discrete integration of the acceleration rate (a) and rotation rate (ω) as following:

$$p(k) = p(k-1) + T \times v(k-1) + \frac{1}{2}T^2 \times a(k-1) \quad (1)$$

$$v(k) = v(k-1) + T \times a(k-1) \quad (2)$$

$$\theta(k) = \theta(k-1) + T \times \omega(k) \quad (3)$$

where T is the sampling time between consecutive time steps.

This navigation information can be measured from various electronic navigational sensors. For example, a GPS can provide absolute measurements of the USV's current location in longitude and latitude, an Inertial Measurement Unit (IMU), which is composed of an accelerometer and a gyroscope, can accurately measure the USV's acceleration and angular velocity over short periods, and an electronic compass is able to provide absolute measurements of the USV's headings. The absolute measurements obtained from
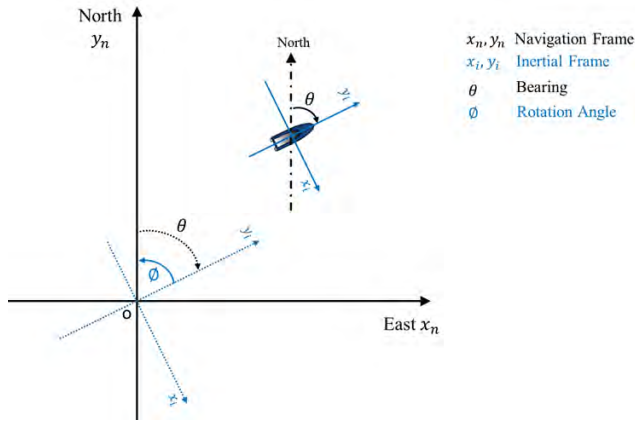
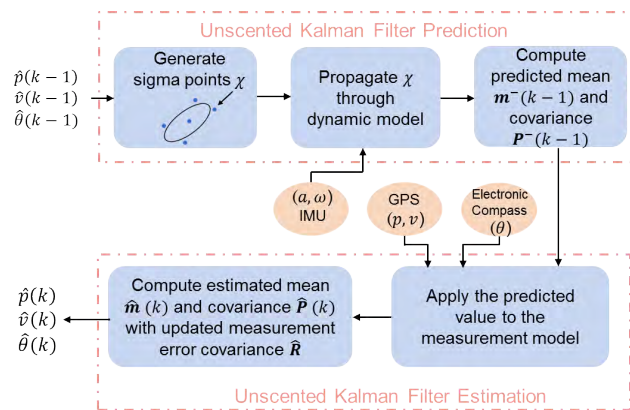**FIGURE 1.** Conversion between different frames.

FIGURE 2. Framework of the proposed data fusion algorithm based on Unsigned Kalman Filter.

the GPS and electronic compass are along the earth frame and can be converted to a pre-defined navigation frame. In contrast, the acceleration rates provided by the IMU are along the inertial frame or the body frame for simplicity and need to be converted to the same navigation frame. Fig. 2 describes these three frames. The pre-defined navigation frame uses the y axis to denote the north direction and the x axis to denote the east direction. The inertial frame can be approximated to the body frame as long as the inertial sensors are installed at the center of the gravity of the USV. The IMU data can then be converted by applying the rotation matrix.

$$\begin{bmatrix} a_{nx} \\ a_{ny} \end{bmatrix} = \begin{bmatrix} cos\emptyset & -sin\emptyset \\ sin\emptyset & cos\emptyset \end{bmatrix} \begin{bmatrix} a_{ix} \\ a_{iy} \end{bmatrix} \qquad (4)$$

where $\emptyset$ is the angle between the body frame (inertial frame) and the navigation frame, and is equal to the USV's heading; a_n is the acceleration in the navigational frame and a_i is that in the inertial frame.

However, precise measurements are not always obtainable in practice due to equipment limitations and environmental influences. A low cost IMU is normally a Micro Electro Mechanical System (MEMS) based sensor, which is sensitive to the surrounding environment, such as dynamic changes and

vibration. Therefore, as stated in (5) and (6), the readings of the accelerometer (a_o) and gyroscope (ω_o) are composed of the true value (a_i, ω_i) and the noise which comprises a constant bias (b_a, b_g) and a random noise (w_a, w_g). The constant bias is varied in different environments and can be determined by a calibration process prior to operation of the USV. The random noise is normally assumed to be white noise.

$$a_o = a_i + b_a + w_a \qquad (5)$$
$$\omega_o = \omega_i + b_g + w_g \qquad (6)$$

The GPS measurements are relatively accurate as long as the receiver is positioned in an open and clear area, where it can access more satellites. That is, it will suffer signal loss or inaccurate measurement in obscured environments. According to Hightower and President [19], in the dynamic environment, the GPS receiver provides constantly changing measurements and this can consequently increase the uncertainty of the measurement error. Although the electronic compass could provide the most accurate measurements, e.g. less than 1°, the distortion of the Earth's magnetic field by nearby ferrous effects, sensor noise and magnetic interferences still have a large impact on the compass during operation. Generally, the measurements from GPS (p_o) and electronic compass (θ_o), which gives the absolute measurements, are modelled by the true value (p_i, θ_i) plus a random white noise (v_p, v_θ) as follows:

$$p_o = p_i + v_p \qquad (7)$$
$$\theta_o = \theta_i + v_\theta \qquad (8)$$

Therefore, data fusion algorithms have to be applied to detect and reduce the possible measurement errors of these complementary sensors during operation.

III. UNSCENTED KALMAN FILTER
The Kalman filter (KF) is a linear recursive data processing algorithm that estimates the real-time state of a system, based upon 1) the initial values of system states; 2) the system and measurement dynamic models; 3) *a priori* knowledge of statistical characteristics of the system noise, such as uncertainties in system dynamic models and measurements [20]. If the input data fits the predefined linear dynamics and statistical models and *a priori* knowledge is known, then the KF can provide, in a minimum variance sense, an optimal estimate of the state vector [21]. Hence, the KF has become the most common technique for estimating the state of a linear system, particularly in navigation systems.

Considering a non-linear system that describes the USV's movement with the discrete system state vector x as:

$$x(k) = f(x(k-1), \quad w(k-1)) \qquad (9)$$

with a measurement

$$z(k) = Hx(k) + v(k) \qquad (10)$$

where $w(k)$ is the process noise and $v(k)$ is the measurement noise. They are both assumed to be white noise with normal probability distribution $p(w) \sim N(0, Q)$ and $p(v) \sim N(0, R)$.

Equations (1) - (3) provide the prediction model of the USV's navigational data and can be viewed as the state equations with p, v and θ being the state of the system, which are the estimation objects of the UKF. Therefore, the state vector x with required data can be defined as:

$$x = \begin{bmatrix} p_x & p_y & v_x & v_y & \theta \end{bmatrix}^T \tag{11}$$

By subscribing the frame conversion (4) into the state equations (1) to (3), the nonlinear dynamic model of the system can then be obtained by (12):

$$f'(x) = \begin{pmatrix} \dot{p}_x \\ \dot{p}_y \\ \dot{v}_x \\ \dot{v}_y \\ \dot{\theta} \end{pmatrix} = \begin{pmatrix} v_x \\ v_y \\ cos\theta a_{ix} - sin\theta a_{iy} \\ sin\theta a_{ix} + cos\theta a_{iy} \\ \omega \end{pmatrix} \tag{12}$$

where p_x and p_y represent the USV's positions in the northeast navigation frame, v_x and v_y are its velocity components and θ is the heading of the USV.

With the absolute measurements of the USV's position and heading from GPS and electronic compass, the measurement transition matrix H can be written as below:

$$H = \begin{bmatrix} 1 & 0 & 0 & 0 & 0 \\ 0 & 1 & 0 & 0 & 0 \\ 0 & 0 & 0 & 0 & 1 \end{bmatrix} \tag{13}$$

The Unscented Kalman Filter (UKF) is a modification of the conventional KF to handle non-linear processes of the predefined system. It has the same fundamental as the conventional KF and involves two steps in the process, prediction and estimation. The framework of this algorithm is illustrated in Fig. 2, where the working process of the UKF has been divided into two parts, namely the UKF prediction module and estimation module.

In the prediction module, the algorithm first uses the unscented transformation to form a set of $2n + 1$ weighted points (Sigma points), where n is the number of the system vector x. All the Sigma points are then propagated through the nonlinear dynamic model yielding the prediction of the next state of the system by assigning different weights to each Sigma point. The algorithm then estimates the optimal next state by estimating the Minimum Mean Square Error (MMSE) of the sensor measurements and predictions. After the optimal estimation, the system will update its covariance matrix to iterate the system and the error covariance of the system will be reduced. The numeric interpretation of this prediction-estimation process is demonstrated in the Appendix.

IV. ADAPTIVE ESTIMATION

Due to the nature of Kalman filtering, the performance of an UKF based multi-sensor data fusion algorithm depends on the statistical system noise, which in practical applications have unrealistic fixed values consequently degrading the performance. In this study a fuzzy logic based adaptive method has been added to the UKF algorithm to match its theoretical and actual noise covariance in real-time (Fig. 3). By using such a method, the measurement noise covariance R can be more robustly estimated, which improves the performance of the multi-sensor data fusion algorithm to determine the locations of the USV.
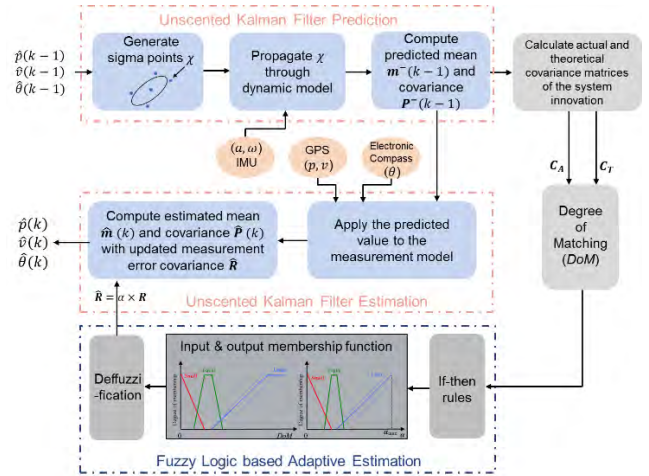

FIGURE 3. Framework of the Adaptive Unscented Kalman Filter data fusion Algorithm.

As shown in Fig. 3, the theoretical covariance C_T and the actual covariance C_A of the innovation sequence ϵ, which is defined as the difference between the measurement z and system prediction x^- (14), are calculated and their similarity is the input of the fuzzy logic system. The system then adjusts the C_T to match the C_A by tuning the UKF measurement noise covariance R.

$$\epsilon(k) = z(k) - Hx^-(k) \tag{14}$$

The theoretical covariance C_T can be computed by the UKF equations (Appendix) as:

$$C_T(k) = HP^-(k)H^T + R \tag{15}$$

where P^- is the predicted covariance, R is the predefined measurement noise covariance. R is commonly defined by the sensor noise characteristics and can be obtained from sensor specifications. In this research, the measurements are provided by GPS positions and compass headings and the measurement noise covariance can be expressed by using the GPS and compass noise as the diagonal value as shown in (16):

$$R = \begin{bmatrix} r_{gpsx}^2 & 0 & 0 \\ 0 & r_{gpsy}^2 & 0 \\ 0 & 0 & r_{com}^2 \end{bmatrix} \tag{16}$$

For a dynamic system, the actual covariance of innovation $C_A(k)$ can be computed as the mean of previous innovations over a moving window size N in a recursive manner:

$$C_A(k) = \frac{1}{N} \sum_{j=k-N+1}^{k} (\epsilon(j)\epsilon(j)^T) \tag{17}$$

$$C_A(k) = C_A(k-1) + \frac{1}{N}\left[(\epsilon(k)\epsilon(k)^T) - (\epsilon(k-N+1)\epsilon(k-N+1)^T)\right] \tag{18}$$

At each time step k, if the fixed value of the measurement noise covariance matrix R is close to the actual measurement noise covariance, it will make the theoretical covariance of innovation C_T equal to the actual covariance of innovation C_A. However, in real applications, sensor disturbances could make C_A differ from C_T, and to improve the performance of UKF, $R(k)$ should be adjusted to reduce the difference between C_T and C_A, which is known as covariance matching. The simplest way to obtain the adjusted $\widehat{R}$ is to let the two covariances equal to each other, so that the updated $\widehat{R}$ can be computed in (19).

$$\widehat{\boldsymbol{R}}(k) = \boldsymbol{C_A}(k) - \boldsymbol{H}\boldsymbol{P}^-(k)\boldsymbol{H}^T \qquad (19)$$

During the calculations of the data fusion algorithm for a practical application, this subtraction equation (19) may generate negative outcomes that would lead to system errors. To correct this, a fuzzy logic based adaptive estimation algorithm has been designed to avoid the possible system error and improve the localization system robustness. The designed fuzzy system employs the similarity of C_A and C_T as its input, which is expressed as multifactor Degree of Matching (DoM) in this paper with the definition as:

$$\boldsymbol{DoM}(k) = \boldsymbol{C_A}(k)/\boldsymbol{C_T}(k) \qquad (20)$$

Based upon the DoM, the fuzzy logic based algorithm then outputs an adjustment coefficient α to update the measurement noise covariance R using (21).

$$\widehat{\boldsymbol{R}}(k) = \boldsymbol{\alpha}(k) \times \boldsymbol{R}(k) \qquad (21)$$

In general, the relationship between the coefficient α and DoM can be described as following:

If $DoM > 1$, C_A is larger than C_T, R should be increased to reduce the two innovation covariance matrices, then α should be larger than 1;

If $DoM \sim= 1$, C_A is similar to C_T, then α should equal to 1 to maintain R unchanged;

If $DoM < 1$, C_A is smaller than C_T, R should be deceased, then α should be reduced to be smaller than 1.

The fuzzy rules with thresholds ($ep1$ and $ep2$) can then be defined based on the relationship between α and DoM in Table 1. The thresholds $ep1$ and $ep2$ are two small values used to create intersections between each fuzzy rule that allows the algorithm to compute the adjustment coefficient α in a fuzzy way.

TABLE 1. Fuzzy rules.

Rule 1: If $DoM > 1 + ep2$, then α is large;
Rule 2: If $1 - ep1 \le DoM \le 1 + ep1$, then α is equal;
Rule 3: If $DoM < 1 - ep2$, then α is small.

The range of DoM at each time step k is divided into six bands to define the following input membership functions of the fuzzy system.

Large:

$$\mu_l = \begin{cases} 1 & DoM > max \\ \dfrac{1 + ep2 - DoM}{ep2 + 1 - max} & 1 + ep2 < DoM \le max \end{cases} \qquad (22)$$

Equal:

$$\mu_e = \begin{cases} \dfrac{1 + ep1 - DoM}{ep1 - ep2} & 1 + ep2 < DoM \le 1 + ep1 \\ 1 & 1 - ep2 < DoM \le 1 + ep2 \\ \dfrac{DoM + ep1 - 1}{ep1 - ep2} & 1 - ep1 \le DoM \le 1 - ep2 \end{cases} \qquad (23)$$

Small:

$$\mu_s = \dfrac{1}{ep2 - 1} \times DoM + 1 \quad DoM < 1 - ep2 \qquad (24)$$

Based on the fuzzy rules, the output membership functions can then be determined as follows:

Large:

$$o_l = \dfrac{1 + al\_ep2 - \alpha}{al\_ep2 + 1 - al\_max} \quad \alpha > 1 + al\_ep2 \qquad (25)$$

Equal:

$$o_e = \begin{cases} \dfrac{1 + al\_ep1 - \alpha}{al\_ep1 - al\_ep2} & 1 + al\_ep2 < \alpha \le 1 + al\_ep1 \\ 1 & 1 - al\_ep2 < \alpha \le 1 + al\_ep2 \\ \dfrac{\alpha + al\_ep1 - 1}{al\_ep1 - al\_ep2} & 1 - al\_ep1 < \alpha \le 1 - al\_ep2 \end{cases} \qquad (26)$$

Small:

$$o_s = \dfrac{1}{al\_ep2 - 1} \times \alpha + 1 \quad \alpha < 1 - al\_ep2 \qquad (27)$$

Then, at each sampling time step k, the adjustment coefficient α is defuzzified by applying a Centroid method where multiple rules can be applied as:

$$\alpha = \dfrac{\int o_i(\alpha)\, \alpha\, d\alpha}{\int o_i(\alpha)\, d\alpha} \quad i = l, e, s \qquad (28)$$

V. SIMULATIONS

In order to simulate an USV operation in a practical environment, waypoint tracking missions have been assigned to the USV according to the map of its surrounding environment. At the start point, the simulated USV calculates the distance and bearing to the next waypoint in real time to verify whether it reaches a predesigned waypoint, which is called waypoint clearance. The condition for a waypoint clearance is:

$$\left| p_{USV} - p_{wp} \right| < d \qquad (29)$$

where p_{USV} is the current position of the USV, p_{wp} is the position of the target waypoint, d is the predesigned minimum target radius around the waypoint. The USV can be considered as having reached the waypoint by entering a circle with radius d around the waypoint. According to the
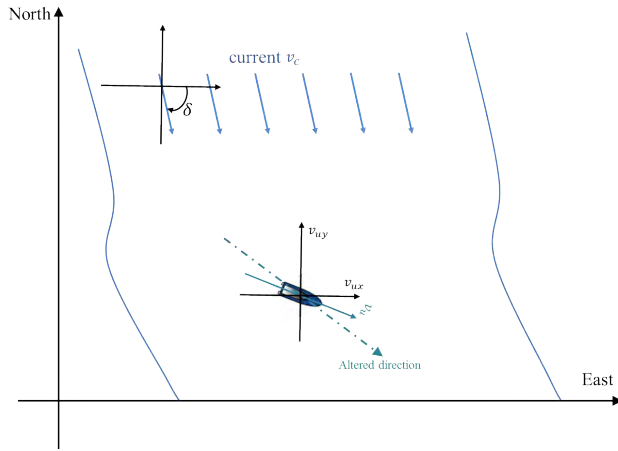
FIGURE 4. Calculation of Tidal effect to the USV speed.

FIGURE 5. Simulation environment in Solent: (a) shows the satellite map with planed waypoint tracking trajectory of the USV, a variant current is simulated along the coastline; (b) gives the binary map that converted from the satellite map with the drifted trajectory of the USV caused by the variant current.

waypoint clearance condition, the operation of the USV will be adjusted by changing its heading so as to track the target waypoint. Once the conditions are met, which indicates that the USV has reached the waypoint, it will start calculating its current distance and bearing to the next predesigned waypoint and keep repeating the waypoint clearance procedure until it reaches the final destination.

The simulations have been carried out based on an actual environment being in the Solent, Southampton, UK (Fig. 5(a)). According to Townend from the environment agency Defra [22], in the Southampton area, the tidal current at the mouth has a peak speed of 0.7 m/s on the flood and 1.0m/s on the ebb. Therefore, a constant current speed v_c along the direction of the water flow that would causes drifting of the USV's position is simulated as an environment influence. Fig. 4 shows how the tidal current would affect the USV's trajectory. The velocity (v_r) of the simulated USV with respect to the water should then be computed by the resultant of USV's own velocity (v_u) and effect of the tidal current as shown in (30).

$$\begin{bmatrix} v_{rx} \\ v_{ry} \end{bmatrix} = \begin{bmatrix} v_{ux} + v_c \times cos\,\delta \\ v_{uy} + v_c \times sin\,\delta \end{bmatrix} \qquad (30)$$

where δ is the direction of the water current.

As illustrated in Fig. 5(a), the water current has been simulated at constant speed but in varied directions to match the water flow directions in the area. The flow data of the currents is based upon previous recorded information [23] and tide tables [24] for the tidal currents in the Solent and Southampton water. The mission start point (765m, 728m) is chosen at the top right corner of the environment map.

The USV is simulated to travel along the coastline to the end point (30m, 250m) located at the lower left of the map. Two waypoints (650, 385), (320, 190) are set for the USV to conduct maneuvers so as to complete the mission while avoiding collision risks with the land. The initial velocity and heading of the simulated USV is 1 m/s at 210°. As shown
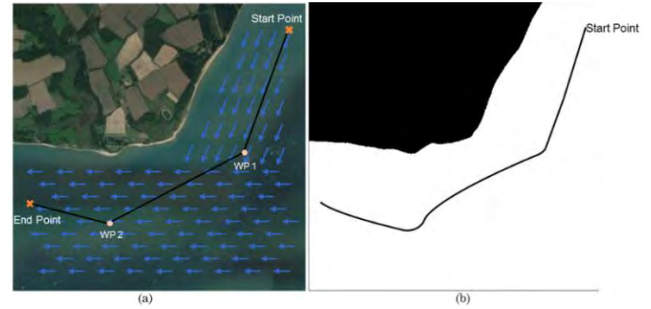
in Fig. 5(b), the planned trajectory is altered by the influence of the water current.

In order to verify the working performance of the modified adaptive UKF algorithm, three scenarios are considered: 1) a system with good knowledge of the *a priori* measurement noise; 2) a system with poor knowledge of the *a priori* measurement noise; 3) a system with good knowledge of the *a priori* measurement noise initially but the actual sensor noise changes during the operation. The UKF noise characteristic and the fuzzy adaptive estimation algorithm thresholds listed in Table 2 remain the same for all the three simulations.

TABLE 2. UKF characteristics and fuzzy system threshold.

Accelerometer noise	$q_{1x} = 0.0039\ m/s^2$
	$q_{1y} = 0.0039\ m/s^2$
Gyroscope noise	$q_2 = 0.033\ deg/s$
GPS noise	$r_{gpsx} = 6\ m$
	$r_{gpsy} = 7\ m$
Compass noise	$r_{com} = 0.5\ deg$
Input Membership	$ep1 = 0.25$
Function	$ep2 = 0.15$
Thresholds	$max = 7$
Output Membership	$al\_ep1 = 0.2$
Function	$al\_ep2 = 0.08$
Thresholds	$al\_max = 5$

A. SIMULATION SCENARIO 1

In this simulation, the noise of sensor measurements are assumed to be predictable based on the Rooted Mean Square Error (RMSE) values in their data sheet, which are close to the predefined UKF error characteristics in Table 2. The simulated sensor errors for the sensor measurement models (shown in equations (5) to (8)) during USV operation are listed in Table 3.

TABLE 3. Simulated sensor noise characteristics.

Sensor	Measurement	Noise	
		Bias	Variance
IMU	Acceleration a_x	$0.03\ m/s^2$	$0.0042\ m/s^2$
	Acceleration a_y	$0.02\ m/s^2$	$0.0042\ m/s^2$
	Rotation rate ω	$0.28\,°/s$	$0.036\,°/s$
GPS	Position p_x	0	$8m$
	Position p_y	0	$7m$
Electronic Compass	Heading θ	0	$0.8°$

FIGURE 6. Simulation scenario 1: the converted binary map with the simulated GPS measurements and fused position results by both conventional UKF and adaptive UKF.

FIGURE 7. Simulation scenario 1: true headings, electronic compass measurements and fused heading results by both conventional UKF and adaptive UKF.

Figs. 6 to 9 show how the conventional UKF and adaptive UKF are able to improve raw measurements of the GPS and subsequently provides robust localization capability. A converted binary map of the simulation area is displayed in Fig.6 with the whole simulated USV true trajectory, shown as the black line, the GPS raw measurements as the blue dots
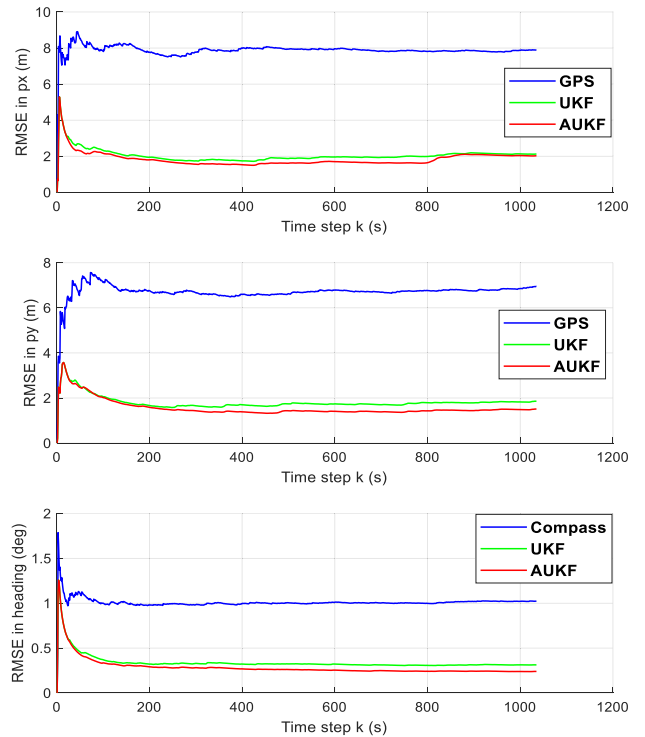

FIGURE 8. Simulation scenario 1: Rooted mean square errors (RMSEs) of the USV's positions and headings.
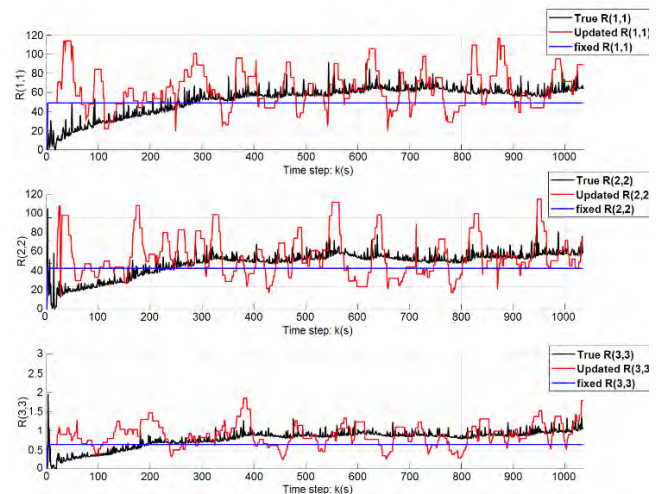

FIGURE 9. Simulation scenario 1: the diagonal elements of the actual, updated and fixed measurement noise covariance matrix.

scattered around the true trajectory subject to the predefined variance, and the fused position results of the conventional UKF and adaptive UKF indicated as green and red lines, respectively. From the enlarged inset in Fig. 6, it is clear that the red line (adaptive UKF result) is slightly closer to the black line compared with the green line (conventional UKF result), which indicates that the proposed adaptive UKF data fusion algorithm performs better when estimating the USV's real-time position than the conventional UKF

algorithm. Fig. 7 demonstrates the USV's heading results, where both conventional and adaptive UKF algorithms are able to reduce the raw compass measurement noise. Again the adaptive UKF algorithm shows marginal improvement in performance. Such a statement can also be supported by Fig. 8, which records the real time RMSEs of the measured and estimated position and heading. The RMSEs of adaptive UKF estimations (red line) are slightly lower than those of the conventional UKF (green line) and they are both much lower than those of the raw sensor measurements. The diagonal elements of the measurement noise covariance matrix R are illustrated in Fig. 9. The true value of the measurement covariance R_a is obtained using (31).

$$\boldsymbol{R_a}(k) = \frac{1}{N} \sum_{j=k-N+1}^{k} (\boldsymbol{v}(j))(\boldsymbol{v}(j))^T \qquad (31)$$

where $\boldsymbol{v}$ is the measurement noise that can be computed by the difference between the sensor measurements $\boldsymbol{z}$ and actual USV navigational data $\boldsymbol{x_a}$ in (32).

$$\boldsymbol{v}(k) = \boldsymbol{z}(k) - \boldsymbol{H}\,\boldsymbol{x_a}(k) \qquad (32)$$

Since the simulated sensor noise are close to the predefined UKF noise characteristics, the actual value of R_a (black line) is close to the fixed value of R (blue line) used in the conventional UKF algorithm. The adjusted $\widehat{R}$ (red line) by the fuzzy adaptive UKF algorithm fluctuates about the actual R_a. This simulation proves the effectiveness of the proposed fuzzy adaptive UKF data fusion algorithm. As long as the system has a good *a priori* knowledge of the sensor measurement noise characteristics, the conventional UKF algorithm is also able to provide accurate estimations of the USV's navigational data even when the USV is operating in a complex environment with turning maneuvers.

B. SIMULATION SCENARIO 2

In a practical environment, sensor measurements accuracy could degrade. During operation sensor noise may be greater than predicted in the sensor manual and differ from UKF predefined noise models that are based on the manuals. In this simulation, poor *a priori* measurement noise has been assigned to the system to verify the performance of the improved fuzzy logic based adaptive estimation algorithm. The RMSE of raw GPS measurements increases to 20m in both x and y axis and the RMSE of the raw compass measurements increases to 5° while the settings of the UKF noise characters are unchanged as shown in Table 2. Such a configuration indicates that the conventional UKF uses the incorrect measurement noise characteristic to make estimations without any update during the process.

Figs. 10 to 13 present the simulation results of the Simulation Scenario 2. Similar to the Simulation Scenario 1, Fig. 10 and Fig. 11 represent the position and heading results of the proposed algorithms together with raw sensor measurements. However, in this simulation, the proposed fuzzy adaptive UKF algorithm performs much better than the conventional UKF. According to the real-time RMSEs for
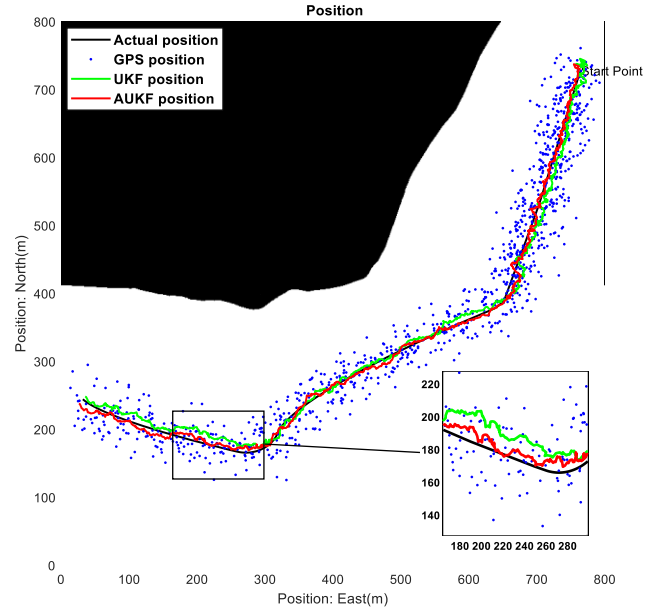

FIGURE 10. Simulation scenario 2: the converted binary map with the simulated GPS measurements and fused position results by both conventional UKF and adaptive UKF.
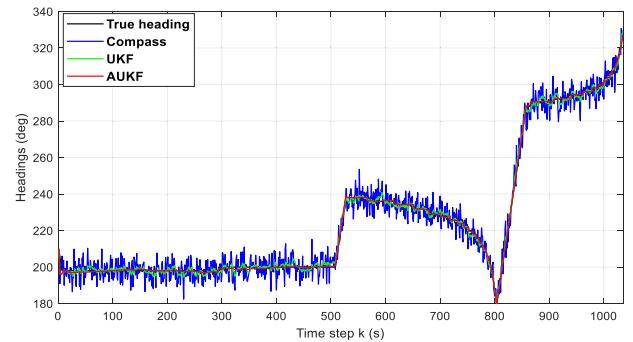

FIGURE 11. Simulation scenario 2: true headings, electronic compass measurements and fused heading results by both conventional UKF and adaptive UKF.

each navigational data processing method shown in Fig. 12, the error of the adaptive UKF estimations are much lower than those of the conventional UKF estimations, providing at least 30% improvement. Such an improvement is due to the fact that the fuzzy adaptive UKF is capable of intelligently calculating the measurement covariance to facilitate improving the accuracy of the filtered data. Fig. 13 demonstrates the diagonal elements of the actual, updated and fixed measurement covariance. The adapted $\widehat{R}$ in this simulation is convergent to the actual R_a when compared to the fixed settings of R.

C. SIMULATION SCENARIO 3

In Simulation Scenario 3, the noise of raw sensor measurements increase during USV operation. During the first 300 time steps, the sensor noise are assumed to be the values used in Simulation Scenario 1. Then sudden changes of sensor noise occur as could occur through unexpected influences
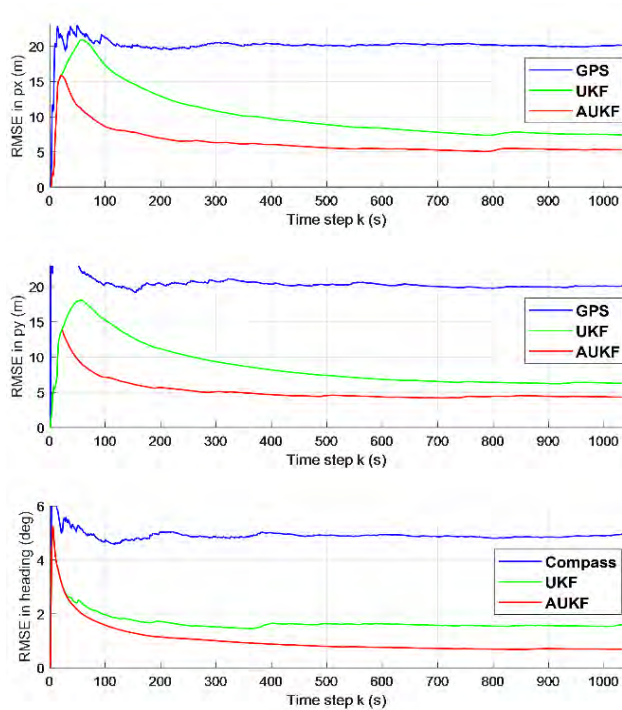
FIGURE 12. Simulation scenario 2: Rooted mean square errors (RMSEs) of the USV's positions and headings.
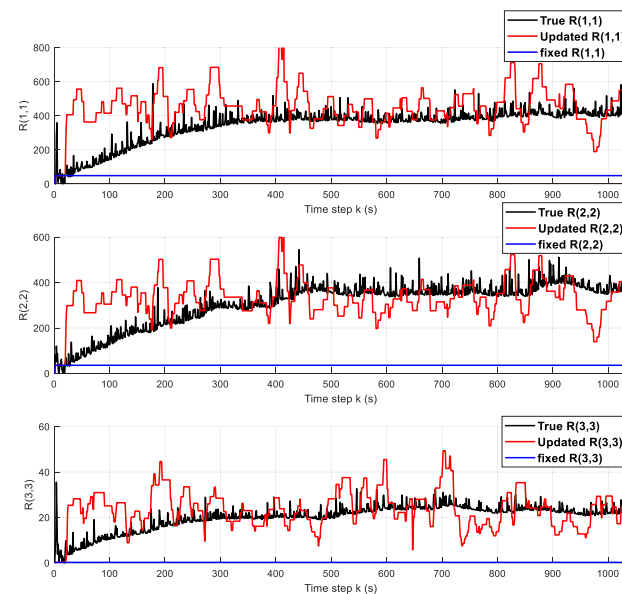

FIGURE 13. Simulation scenario 2: the diagonal elements of the actual, updated and fixed measurement noise covariance matrix.

FIGURE 14. Simulation scenario 3: the converted binary map with the simulated GPS measurements and fused position results by both conventional UKF and adaptive UKF.

FIGURE 15. Simulation scenario 3: true headings, electronic compass measurements and fused heading results by both conventional UKF and adaptive UKF.

on the sensors. The noise are increase to the values used in Simulation Scenario 2. Figures 14 to 17 demonstrates the performance of both the conventional UKF algorithm and the proposed fuzzy adaptive UKF algorithm in this situation. As shown in Fig.14, the GPS measurements become noisier before the first waypoint. The green line that represents the conventional UKF estimated positions starts to fluctuate
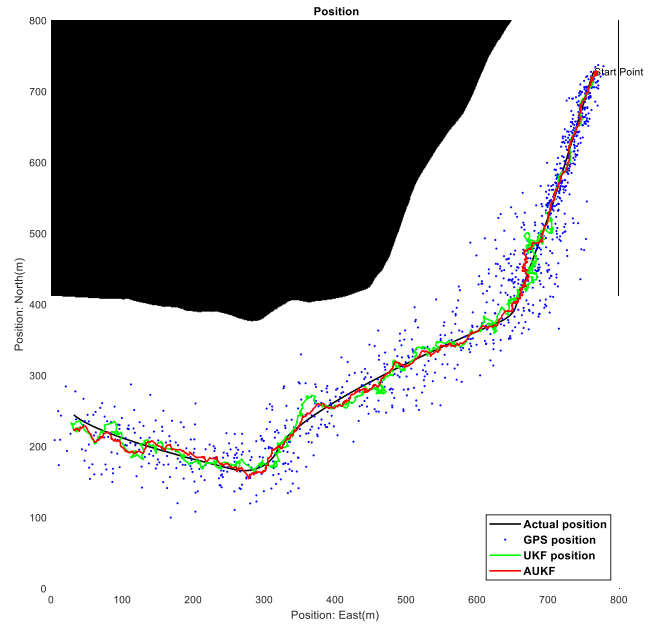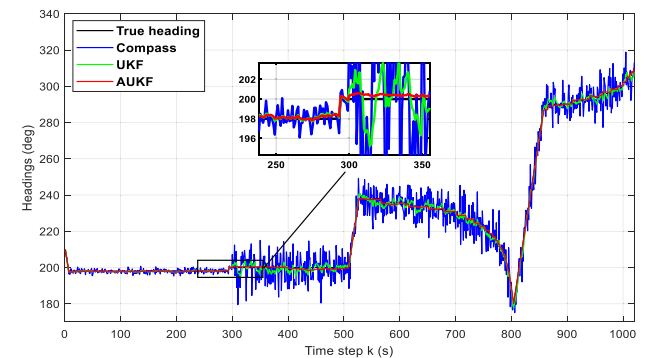
appreciably from the true trajectory (black line) while the adaptive UKF still provides much closer estimations. The better performance of the adaptive UKF algorithm is further proved from the enlarged inset in the heading estimations (Fig. 15). The UKF estimated headings (green line) starts to generate larger errors when the compass error increases, whereas the fuzzy adaptive UKF estimated headings (red line) still maintain their accuracy and report to the true values. The real-time RMSE values of each navigational data processing method further supports that the proposed fuzzy adaptive UKF data fusion algorithm achieves better accuracy when the system is lacking in appropriate *a priori* knowledge of system measurement noise characteristics, even when the sensor noise degrades suddenly. The reason for this is that the proposed algorithm is able to tune the predefined measurement covariance *R* close to the actual value in real-time,
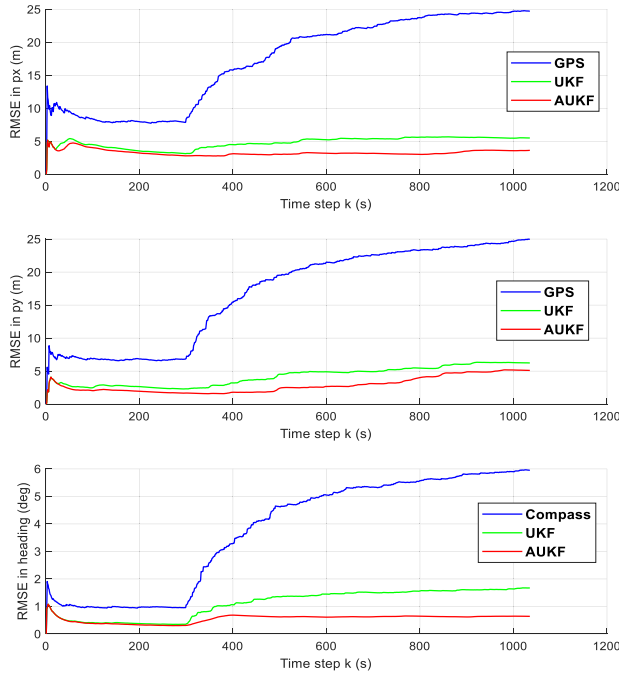
FIGURE 16. Simulation scenario 3: Rooted mean square errors (RMSEs) of the USV's positions and headings.
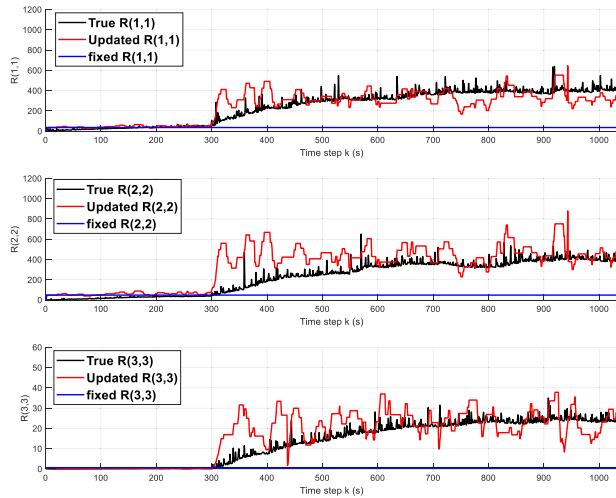

FIGURE 17. Simulation scenario 3: the diagonal elements of the actual, updated and fixed measurement noise covariance matrix.

which is also shown in Fig. 17, instead of fixing it as it is the case with the conventional UKF algorithm.

At this juncture, it can be summarized that in the first simulation, the proposed fuzzy adaptive UKF shows marginal improvement in reducing the raw sensor measurement errors over the conventional UKF. In the second simulation, when the *a priori* information of the sensor noise is poor and largely different to the UKF's settings, the proposed fuzzy adaptive UKF provides more accurate results than the conventional UKF. The improved performance has been demonstrated again in Simulation Scenario 3, where the sensor noise

FIGURE 18. Springer USV developed by MIDAS group from Plymouth University in UK.

changes suddenly during USV operation. The computational time of the proposed multi-sensor data fusion algorithm at each time step in all the three simulations is approximately 0.0023s. It is far below the simulated sampling time of navigation system, of which is 1s. Therefore, the proposed algorithm should be able to conduct data fusion missions in real-time applications.

VI. PRACTICAL TRIAL

To further demonstrate the effectiveness of the proposed method, a field trial using an actual USV has been carried out. The experiment was undertaken through a collaboration program between UCL and Plymouth University to jointly explore the improvement of the autonomous navigation system of a practical USV, *Springer* [25], [26]. The *Springer* USV developed by the Marine and Industrial Dynamic Analysis Research (MIDAS) group (now known as Autonomous Marine Systems Research Group) from the Department of Marine Engineering, Plymouth University is a double hull designed USV, shown in Figure 18. Each hull carries a watertight peli-case that contains the navigational sensors, which are not waterproof, together with a hosting computer. [27], [28]. The *Springer* USV was equipped with all the required sensors, i.e. GPS receiver, IMU, and electronic compass and all the raw measurement data collected during the field test had been recorded. The experiment was held at the Roadford Lake in Devon, UK (Fig. 19) with overcast skies, light precipitation and easterly winds of 1 to 3.2 m/s. Three buoys were set out as the waypoints constituting of a waypoint-tracking path for the *Springer* USV and requiring the USV to make three turning maneuvers to complete the designed mission (Fig. 20). The sampling interval for the sensors to take measurements was 1 second. The duration for one trial is approximately 15 minutes and the USV was operating at a speed of approximately 1.5 m/s.

The actual environment influences such as the wind and water current altered the trajectory of the *Springer* USV, which has been shown in Fig. 21. The blue line represents

FIGURE 19. Experimental environment: Roadford lake, Devon, UK.

FIGURE 20. The satellite map of the Roadford lake and the planned trajectory for the *Springer* USV to follow.

FIGURE 21. The converted binary map with USV's planned trajectory and recorded GPS measurements during the practical experiment.

FIGURE 22. The raw GPS measurements, waypoints positions and estimated positions generated by conventional UKF and adaptive UKF respectively.

raw GPS measurements that have been extracted from the trial. As illustrated in Fig. 21, the USV successfully transited the three waypoints in sequence and returned to the first waypoint as planned, but the water surface currents pushed the vehicle towards the northwest and made large impacts on its trajectory when the USV was facing northeast. As a result, the *Springer* USV turned right first and subsequently made a circular maneuver to alter its direction towards the third buoy instead of directly turning left after it reached the second buoy. This kind of unpredictable event increases the complexity of practical USV operations.

The conventional UKF and the proposed fuzzy adaptive UKF data fusion algorithms are applied to the raw sensor measurements recorded from the practical trial. The average computational time for each cycle of the algorithm is 0.0017s while the actual sensor measurements are sampled at 1s, which confirms the proposed algorithm can be employed in real-time navigation system. The fusion results are plotted in Fig. 22 and Fig. 23. As shown in Fig.22, the red line that denotes the fuzzy adaptive UKF estimated trajectory, is close to the GPS measurements that are represented by the blue line, whereas the green line denotes the conventional
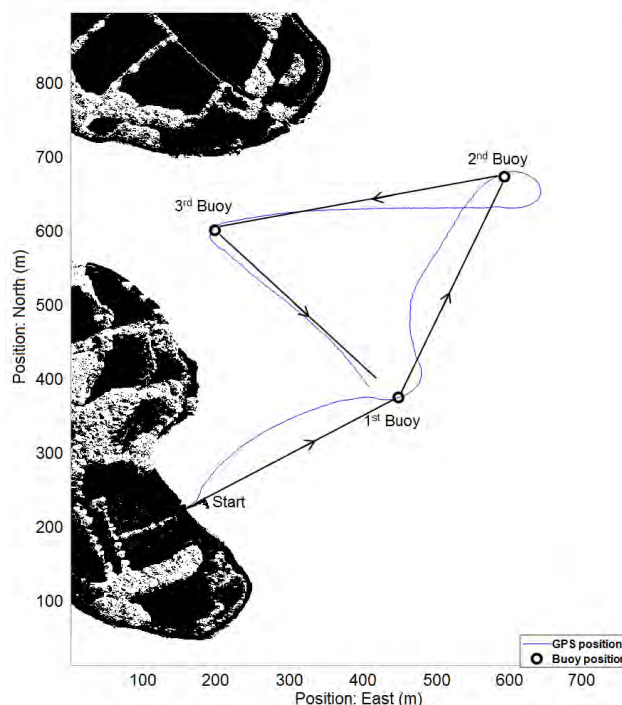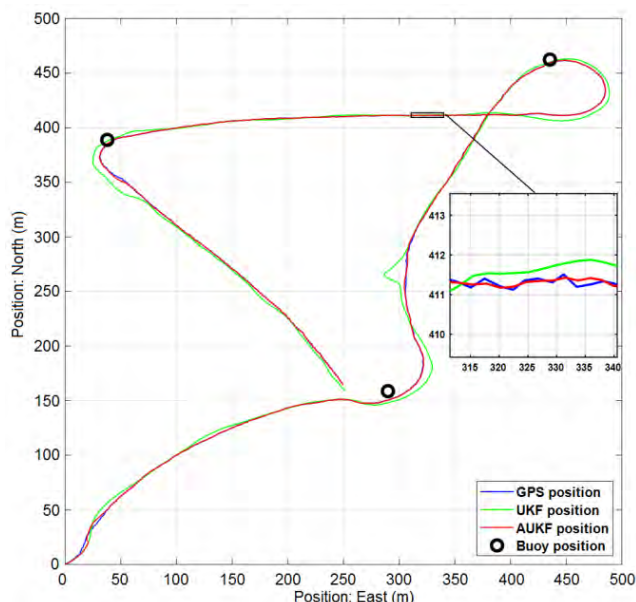
UKF estimated trajectory deviate largely from the other two trajectories. Fig. 23 demonstrates the heading results. It can be seen that the headings estimated by the proposed fuzzy adaptive UKF algorithm (red line) are more coincident with the compass measurement (blue line). Again, the conventional UKF estimations (green line) are associated with deviations from the other two headings. The results validate the
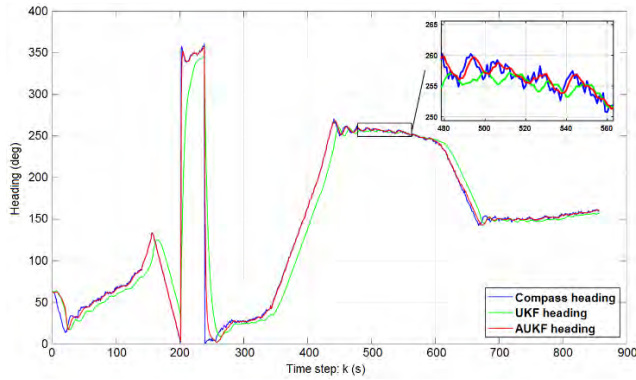
FIGURE 23. The raw compass measurements and estimated headings generated by both conventional UKF and adaptive UKF.

feasibility of the proposed fuzzy adaptive UKF data fusion algorithm whereas the conventional UKF algorithm is prone to error in a practical application. In the simulations, despite the better performance of the proposed fuzzy adaptive UKF algorithm, the conventional UKF can also reduce raw sensor measurement errors. Similar performance that has not been achieved in practice, states the conventional UKF is a theoretical optimal algorithm that provides less satisfactory in practical applications. In the meantime, the real-time adaption of the measurement noise covariance enhances the ability of the proposed fuzzy adaptive UKF algorithm to overcome the unexpected uncertainties in practical applications. Although the true positions and headings of the *Springer* USV are not available in practical trial, the benefits obtained from the proposed algorithm can still be revealed by its smoother estimations with less pinnacles than raw sensors' measurements, which are presented in the enlarged insets in both Fig. 22 and Fig.23.

VII. CONCLUSION

This paper has introduced the development of a new multi-sensor data fusion algorithm for USV navigation in practical complex environments. When considering the environment influences such as water currents, a conventional UKF based algorithm is limited by the lack of capability for dealing with variations in a practical water surface environment. An UKF based multi-sensor data fusion algorithm has therefore been proposed to solve the non-linear issues associated with the navigation system for practical USV applications. A fuzzy adaptive estimation method has been further developed to reduce the effect on the system caused by unknown or unpredicted changes of sensor measurement noise. The fuzzy logic based algorithm determines an adjustment coefficient to adapt the measurement covariance R based on the actual and theoretical innovation covariance matrices of the conventional UKF in real-time. Numerical simulations have been carried out and evaluated in different simulations based upon practical maritime environments and the results illustrate the adaptive estimation based UKF algorithm does improve the accuracy of the conventional

UKF. Although their results are quite similar when the system has accurate noise settings, the adaptive UKF outperforms conventional UKF with observably more accurate position estimations when the system lacks *a priori* knowledge of the sensors' measurement noise; the improvement that can be achieved is approximately 30%. The algorithms are then applied to the actual sensor measurements that are recorded from a practical experiments and the results suggest that this newly developed algorithm delivers a more practical solution to solve the problem of the robust localization of USVs.. This research can be further improved by investigating how the processing noise covariance would affect the performance of the proposed UKF based data fusion algorithm and subsequently designing an improved mathematical method to deal with such effects so that the AUKF algorithm would be more adaptive in practical USV applications.

APPENDIX

Unscented Kalman Filter

Step 1: Prediction

a) Generate $2n + 1$ sigma points ($n = 5$)
$$\chi_0(k - 1) = m(k - 1)$$
$$\chi_i(k - 1) = m(k - 1) + \sqrt{n + \lambda}\left[\sqrt{P_i(k - 1)}\right]$$
$$\chi_{i+n}(k - 1) = m(k - 1) - \sqrt{n + \lambda}\left[\sqrt{P_i(k - 1)}\right], i = 1, \ldots, n$$

The constant weights W_i^m and W_i^c are computed as follows:
$$W_0^m = \lambda/(n + \lambda)$$
$$W_0^c = \frac{\lambda}{(n+\lambda)} + \left(1 - \alpha^2 + \beta\right)$$
$$W_i^m = W_i^c = 1/2\,(n + \lambda), i = 1, \ldots, 2n$$

where $\lambda = \alpha^2\,(n + \kappa) - n$. The parameters α and κ determine the spread of the sigma points around the mean. β describes the distributed information, of which the optimal value is 2 for Gaussian distribution.

b) Propagate the sigma points through the dynamic model
$$\widehat{\chi_i}(k) = f\left(\chi_i(k - 1)\right), i = 0, \ldots, 2n$$

c) Compute the predicted mean $m^-(k)$ and the predicted covariance $P^-(k)$
$$m^-(k) = \sum_{i=0}^{2N} W_i^m \widehat{\chi_i}(k)$$
$$P^-(k) = \sum_{i=0}^{2N} W_i^c \left(\widehat{\chi_i}(k) - m^-(k)\right)\left(\widehat{\chi_i}(k) - m^-(k)\right)^T + Q(k - 1)$$

where N is the dimension of the expended state space, which equals to $N_x + N_w + N_v$. N_x is the dimension of the original state that equals to n; N_w and N_v are the dimensions of white noise w and v.

Step 2: Estimation
$$K(k) = P^-(k)H^T\left[HP^-(k)H^T + R\right]^{-1}$$
$$\widehat{x}(k) = m^-(k) + K(k)\left[z(k) - Hm^-(k)\right]$$
$$P(k) = (I - K(k)H)P^-(k)$$

the experiments. The authors are also indebted to Mr. Konrad Yearwood for his valuable critique of this paper.

REFERENCES

[1] I. M. Pires, N. M. Garcia, N. Pombo, and F. Flórez-Revuelta, "From data acquisition to data fusion: A comprehensive review and A roadmap for the identification of activities of daily living uSING mobile devices," *Sensors*, vol. 16, no. 2, p. 184, Feb. 2016.

[2] F. Castanedo, "A review of data fusion techniques," *Sci. World J.*, vol. 2013, Feb. 2013, Art. no. 704504. [Online]. Available: https://www.hindawi.com/journals/tswj/2013/704504/

[3] S. Sarkka, "Bayesian estimation of time-varying systems: Discrete-time systems," Dept. Elect. Eng. Automat., Aalto Univ., Espoo, Finland, Tech. Rep., 2011.

[4] S. J. Julier and J. K. Uhlmann, "Unscented filtering and nonlinear estimation," *Proc. IEEE*, vol. 92, no. 3, pp. 401–422, Mar. 2004.

[5] E. A. Wan and R. Merwe, "The unscented Kalman filter for nonlinear estimation," in *Proc. IEEE Adapt. Syst. Signal Process., Commun., Control Symp.*, Oct. 2002, pp. 153–158.

[6] P. Zhang, J. Gu, E. E. Milios, and P. Huynh, "Navigation with IMU/GPS/Digital compass with unscented Kalman filter," in *Proc. IEEE Int. Conf. Mechatron. Automat.*, Niagara Falls, Canada, Jul. 2005, pp. 1497–1502.

[7] E. J. Choi, J. C. Yoon, B. S. Lee, S. Y. Park, and K. H. Choi, "Onboard orbit determination using GPS observations based on the unscented Kalman filter," *Adv. Space Res.*, vol. 46, no. 11, pp. 1440–1450, Dec. 2010.

[8] D. Lee, G. Vukovich, and R. Lee, "Robust unscented Kalman filter for nanosat attitude estimation," *Int. J. Control, Autom. Syst.*, vol. 15, no. 5, pp. 2161–2173, Oct. 2017.

[9] S. Sarkka, *Bayesian Filtering and Smoothing*. Cambridge, U.K.: Cambridge Univ. Press, 2013.

[10] C. Hu, W. Chen, Y. Chen, and D. Liu, "Adaptive Kalman filtering for vehicle navigation," *J. Global Positioning Syst.*, vol. 2, no. 1, pp. 42–47, Nov. 2003.

[11] C. Tseng, S. Lin, and D. Jwo, "Fuzzy adaptive cubature Kalman filter for integrated navigation systems," *Sensors*, vol. 16, no. 8, p. 1167, Aug. 2016.

[12] B. Zheng, P. Fu, B. Li, and X. Yuan, "A robust adaptive unscented Kalman filter for nonlinear estimation with uncertain noise covariance," *Sensors*, vol. 18, no. 3, p. 808, Mar. 2018.

[13] X. Wang, Z. You, and K. Zhao, "Inertial/celestial-based fuzzy adaptive unscented Kalman filter with covariance intersection algorithm for satellite attitude determination," *Aerosp. Sci. Technol.*, vol. 48, pp. 214–222, Nov. 2015.

[14] M. Jin, J. Zhao, J. Jin, G. Yu, and W. Li, "The adaptive Kalman filter based on fuzzy logic for inertial motion capture system," *Measurement*, vol. 49, pp. 196–204, Mar. 2014.

[15] A. Rahimi, K. D. Kumar, and H. Alighanbari, "Enhanced adaptive unscented Kalman filter for reaction wheels," *IEEE Trans. Aerosp. Electron. Syst.*, vol. 51, no. 2, pp. 1568–1575, Apr. 2015.

[16] A. Almagbile, J, Wang and W. Ding, "Evaluating the performances of adaptive Kalman filter methods in GPS/INS integration," *J. Global Positioning Syst.*, vol. 9, no. 1, pp33–40, 2010.

[17] Y. S. Meng, S. Gao, Y. Zhong, G. Hu, and A. Subic, "Covariance matching based adaptive unscented Kalman filter for direct filtering in INS/GNSS integration," *Acta Astronautica*, vol. 120, pp. 171–181, May 2016.

[18] M. S. Grewal and A. P. Andrews, *Kalman Filtering: Theory and Practice Using Matlab*, 3rd ed. Hoboken, NJ, USA: Wiley, 2008.

[19] P. Hightower and V. President, "Motion effects on GPS receiver time accuracy," *Instrum. Technol. Syst.*, to be published.

[20] P. Maybeck, *Stochastic Models, Estimation, and Control*, vol. 1, New York, NY, USA: Academic, 1979.

[21] A. Gelb, *Applied Optimal Estimation*. Washington DC, USA: Analytic Sci. Corp., 1974.

[22] I. Townend. (2018). *Supporting Document: A Conceptual Model of Southampton Water*. [Online]. Available: http://www.estuary-guide.net/pdfs/southampton_water_case_study.pdf

[23] N. Coastwatch. (2018). *Solent Tides and Currents*. [Online]. Available: https://www.nci.org.uk/stations/solent-tides-and-currents

[24] D. Dolby. (2018). *Lee-On-The-Solent Tide Times*. [Online]. Available: www.tidetimes.org.uk

[25] R. Song, Y. Liu, and R. Bucknall, "Smoothed A* algorithm for practical unmanned surface vehicle path planning," *Appl. Oceans Res.*, vol. 83, pp. 9–20, 2019.

[26] A. Motwani, W. Liu, S. Sharma, R. Sutton, and R. Bucknall, "An interval Kalman filter-based fuzzy multi-sensor fusion approach for fault-tolerant heading estimation of an autonomous surface vehicle," *J. Eng. Maritime Environ.*, to be published.

[27] M. Group and P. University. (Nov. 2018). *Springer Unmanned Surface Vehicle*. [Online]. Available: http://www.tech.plymouth.ac.uk/sme/springerusv

[28] R. Sutton, S. Sharma, and T. Xu, "Adaptive navigation systems for an unmanned surface vehicle," *J. Marine Eng. Technol.*, vol. 10, no. 3, pp. 3–20, Sep. 2011.

WENWEN LIU received the B.Eng. degree in electrical and electronic engineering from Northumbria University, Newcastle upon Tyne, U.K., in 2011, and the M.Sc. degree in power systems engineering from University College London, London, U.K., in 2012. She is currently pursuing the Ph.D. degree with University College London, London. Her research interest includes developing robust multi-sensor data fusion algorithms for Unmanned Surface Vehicle (USV) navigation and target detection.

YUANCHANG LIU received the B.Eng. degree in control engineering from the Dalian University of Technology, in 2010, the M.Sc. degree in power systems engineering, and the Ph.D. degree in marine control engineering from University College London, in 2011 and 2016, respectively, where he is currently a Lecturer with the Department of Mechanical Engineering. Before joining the department, he was a Research Fellow in robotic vision and autonomous vehicles of the Surrey Space Centre, University of Surrey. His research focuses on automation and autonomy, with a special interest in the exploration of technologies for sensing and perception, and guidance and control of intelligent and autonomous vehicles. He is currently supervising four Ph.D. students, working on the project of autonomous navigation for unmanned marine vehicles.

RICHARD BUCKNALL is currently a Professor of marine systems with the Department of Mechanical Engineering, University College London (UCL), and a Visiting Professor in marine systems with the Stevens Institute of Technology, Hoboken, NY, USA. Having gained experience working in both the shipping and rail industries as a practicing engineer across the world, he joined UCL as a Researcher, in 1995, and was promoted to Professor, in 2012. His research interests are in exploiting technologies in the transport sector, examining how new technologies should be developed and will impact the design and operation of new vehicles, and is currently interested in unmanned surface vessels. He is currently working on the autonomous operation of vehicles with a particular interest in unmanned surface vessels. He is running many projects that support two Research Assistants and 10 Ph.D. studentships.

• • •